This document is confidential and is proprietary to the American Chemical Society and its authors. Do not copy or disclose without written permission. If you have received this item in error, notify the sender and delete all copies.

# Proton-coupled Electron Transfer in a Ruthenium (II) Bipyrimidine Complex in its Ground and Excited Electronic States

Journal:	The Journal of Physical Chemistry
Manuscript ID	Draft
Manuscript Type:	Article
Date Submitted by the Author:	n/a
Complete List of Authors:	Drummer, Matthew; University of Illinois at Chicago, Department of Chemistry; Argonne National Laboratory Weerasooriya, Ravindra; University of Illinois at Chicago, Department of Chemistry; Argonne National Laboratory Gupta, Nikita; University of Illinois at Chicago, Department of Chemistry; Argonne National Laboratory Askins, Erik; University of Illinois at Chicago, Department of Chemistry; Argonne National Laboratory Liu, Xiaolin; University of Washington, Chemistry Valentine, Andrew; University of Washington, Chemistry Li, Xiaosong; University of Washington, Department of Chemistry Glusac, Ksenija; University of Illinois at Chicago, Department of Chemistry; Argonne National Laboratory

SCHOLARONE™ Manuscripts

# Proton-coupled Electron Transfer in a Ruthenium (II) Bipyrimidine Complex in its Ground and Excited Electronic States

Matthew C. Drummer<sup>1,2</sup>, Ravindra B. Weerasooriya<sup>1,2</sup>, Nikita Gupta<sup>1,2</sup>, Erik J. Askins<sup>1,2</sup>, Xiaolin Liu<sup>3</sup>, Andrew J. S. Valentine<sup>3</sup>, Xiaosong Li<sup>3</sup>, and Ksenija D. Glusac<sup>1,2</sup>

<sup>1</sup>Department of Chemistry, University of Illinois at Chicago, Chicago, Illinois 60607, United States

<sup>2</sup>Chemical Sciences and Engineering, Argonne National Laboratory, Illinois 60439, United States

<sup>3</sup>Department of Chemistry, University of Washington, Seattle, Washington 98195-1700, United States

#### Abstract

Proton-coupled electron transfer (PCET) was studied for the ground and excited electronic states of a [Ru(terpy)(bpm)(OH<sub>2</sub>)(PF<sub>6</sub>)<sub>2</sub>] complex, **Ru-bpm**. Cyclic voltammetry measurements show that the Ru(II)-aqua moiety undergoes PCET to form a Ru(IV)-oxo moiety in the anodic region, while the bpm ligand undergoes PCET to form bpmH<sub>2</sub> in the anodic region. The photophysical behavior of **Ru-bpm** was studied using steady-state and femtosecond transient UV-vis absorption spectroscopy, coupled with density functional theory (DFT) calculations. The lowestlying excited state of **Ru-bpm** is described as a (Ru  $\rightarrow$  bpm) metal-to-ligand charge transfer (MLCT) state, while the metal-centered (MC) excited state was found computationally to be close in energy to the lowest-energy bright MLCT state (MC state was 0.16 eV above the MLCT state). The excited state kinetics of **Ru-bpm** were found via transient absorption spectroscopy to be short-lived and were fit well to a biexponential function with lifetimes  $\tau_1$ =4 ps and  $\tau_2$ =65 ps in aqueous solution. Kinetic isotope effects of 1.75 ( $\tau_1$ ) and 1.61 ( $\tau_2$ ) were observed for both decay components, indicating that the solvent plays an important role in the excited-state dynamics of Ru-bpm. Based on the pH-dependent studies and the results from prior studies of similar Rucomplexes, we hypothesize that the <sup>3</sup>MLCT state forms an excited-state hydrogen-bond adduct with the solvent molecules and that this process occurs with a 4 ps lifetime. The formation of such hydrogen-bond complex is consistent with the electronic density accumulation at the peripheral N atoms of the bpm moiety in the <sup>3</sup>MLCT state. The hydrogen-bonded state <sup>3</sup>MLCT' decays to the ground state with a 65 ps lifetime. Such a short lifetime is likely associated with the efficient vibrational energy transfer from the <sup>3</sup>MLCT state to the solvent.

#### **Keywords**

Ruthenium, polypyridyl, bipyrimidine, terpyridine, transient absorption spectroscopy, cyclic voltammetry, density functional theory, metal-to-ligand charge-transfer, metal-centered, short-lived excited state, PCET.

## Corresponding author's email

glusac@uic.edu

#### Introduction

Ruthenium-based transition metal complexes, particularly Ru(II) polypyridyl motifs, exhibit attractive photophysical and photochemical properties due to the presence of many excited-state electronic configurations which are governed by ligand coordination. 1-3 In general, three types of low-lying excited states are present in these complexes, namely metal-to-ligand-charge transfer (MLCT), metal-centered (MC) and ligand-centered (LC) states. Recent two-dimensional spectroscopic studies have pinpointed Ru-N and other vibrational states responsible for internal conversion between different excited states in a Ru-polypyridine complex.<sup>4</sup> The relative energy order of the excited states depends on the ligand field strength and its standard reduction potential. In homoleptic Ru-polypyridyl complexes, polarization-dependent experiments have shown that the excited electron in the initial Franck-Condon state is delocalized over all ligands.<sup>5</sup> However, the interactions of the chromophore with solvent molecules leads to rapid decoherence and localization of the electronic density on one of the ligands. Due to the Ru heavy-atom effect, intersystem-crossing rates in Ru-complexes are large and the triplet excited states are often formed within the first hundred femtoseconds after photoexcitation. The complexes with lowest-energy <sup>3</sup>MLCT states tend to have long excited-state lifetimes and decent photostability, while the presence of close-lying MC states generally shortens the lifetimes and leads to ligand dissociationbased photochemistry.<sup>2</sup> As the ligand conjugation is increased, the long-lived triplet LC states tend to dominate the photophysical behavior of Ru-polypyridyl complexes.<sup>6,7</sup>

Terpyridine (terpy) Ru(II) complexes tend to exhibit relatively short excited-state lifetimes.<sup>8</sup> For example, the lifetime of Ru(terpy)<sub>2</sub><sup>2+</sup> is only 250 ps,<sup>9</sup> and this behavior has been attributed to the unfavorable bite angle of the terpy ligand, which weakens the ligand field in Ru-terpy complexes. One consequence of this is weak splitting of d orbitals and a lowering of MC ( $\pi(t_{2g}) \rightarrow *\sigma(e_g)$ ) state energies. For example, variable-temperature emission spectroscopy revealed that the <sup>3</sup>MC state in Ru(terpy)<sub>2</sub><sup>2+</sup> is only 0.2 eV above the <sup>3</sup>MLCT ( $\pi(t_{2g}) \rightarrow *\pi(terpy)$ ) state,<sup>10</sup> while the corresponding energy difference in Ru(bpy)<sub>3</sub><sup>2+</sup> is 0.5 eV.<sup>11</sup> These energy differences are also consistent with DFT-calculated values.<sup>12</sup> The lifetime of bis(tridentate) Ru(II) complexes can be improved either using tridentate ligands with improved bite angles<sup>13</sup> or by incorporation of strong  $\sigma$ -donating ligands.<sup>14</sup>

The redistribution of electron density in MLCT excited states often modulates the pKa values of Ru-based complexes, leading to proton-coupled processes. In general, acid/base groups will become either more acidic due to the electronic density depletion at the metal center in the MLCT states, or more basic due to the accumulation of the electronic density at the accepting ligand orbital of the MLCT state. As a consequence, the acid/base groups located on the ligand that is not directly involved in the MLCT state will become more acidic in the excited state. For example, the cyano ligands in Ru(bpy)2(CN)2 possess basic nitrogen atoms with a ground-state pKa value of 0.12. In the Ru(d)  $\rightarrow$  bpy( $\pi^*$ ) MLCT state, the pKa value of the protonated cyano group shifts to a value of pKa\*=-5.7, reflecting the significant electronic depletion on the neighboring Ru center. On the other hand, the acid/base groups located on the ligand that accepts the electronic density upon MLCT excitation will become more basic. On the ligand that accepts

Here, we report an investigation of electronic properties of a Ru-based complex, **Ru-bpm**, that contains a bipyrimidine ligand capable of accepting electrons and protons under applied potential

or visible light photoexcitation (Scheme 1). Electrochemical, spectroscopic, and computational studies were utilized to investigate the ground and excited-state electron and proton transfer chemistry of **Ru-bpm**. From cyclic voltammetry, we find the presence of metal-centered and ligand-centered PCET processes in anodic and cathodic regions, showing the richness of the redox properties of **Ru-bpm**. The excited state behavior of **Ru-bpm** was found to be dominated by a Ru  $\rightarrow$  bpm MLCT state which was surprisingly short-lived (decaying on the picosecond timescale). A detailed pH-dependent study revealed that the most likely reason for the fast excited-state deactivation in **Ru-bpm** is the formation of a hydrogen-bonded complex with the surrounding solvent molecules which causes an increased rate of nonradiative decay via vibrational energy transfer to the solvent.

#### **Methods**

**Materials and methods.** All chemicals and solvents were purchased from commercial suppliers and used without further purification unless otherwise noted. <sup>1</sup>H NMR spectra were collected using a Bruker Avance III HD operating at 11.74 T, 500 MHz. Mass spectra were collected via electrospray ionization mass spectrometry using a Waters Synapt G2-Si ESI mass spectrometer. **Ru-bpm** was synthesized according to the previously published procedure. <sup>25</sup> MS-ESI: m/z (CH<sub>3</sub>CN) 528 ([M–PF<sub>6</sub>]<sup>+</sup>), <sup>1</sup>H NMR (500 MHz, CD<sub>3</sub>CN) δ (ppm): 10.81 (s, 1H), 9.26 (d, 1H), 8.64 (m, 2H), 8.52 (m, 2H), 8.39 (m, 2H), 8.35 (m, 1H), 8.15 (m, 2H), 7.92 (m, 2H), 7.68 (d, 2H), 7.27 (t, 2H). Steady-state UV-vis absorption was measured using a Thermo Scientific Evolution 201 UV-vis spectrophotometer with samples placed in a 2 mm quartz cuvette for initial steady-state and subsequent transient absorption measurements. For the pH-dependent study, samples were measured in 1cm quartz cuvettes.

**Electrochemistry.** Cyclic voltammetry (CV) measurements of the **Ru-bpm** were performed in a standard three-electrode cell consisting of a glassy carbon (GC, MF-2012, Bioanalytical systems, 0.075 cm<sup>2</sup> surface area) working electrode, 3M Ag/AgCl aqueous reference electrode (MF-2052, Bioanalytical systems) and Pt wire counter electrode (MW-4130, Bioanalytical systems). The CV measurements were performed at 1 mM **Ru-bpm** concentrations in aqueous 1 M phosphate solutions in the pH 2-12 region. At highly acidic (pH  $\leq$  1) and basic (pH  $\geq$  13) pHs, solutions were made with HClO<sub>4</sub> and NaOH, respectively. Each working electrode was polished before each measurement with alumina (CF-1050, Bioanalytical systems) and diamond (MF-2054, Bioanalytical systems) slurry. All the potentials shown are referenced against the normal hydrogen electrode (NHE).

**Transient absorption spectroscopy.** Femtosecond transient absorption spectroscopy was done using a setup consisting of a mode-locked Ti:sapphire laser and regenerative amplifier (Astrella, Coherent Inc.) operating at a repetition rate of 1 kHz to generate a 100 fs pulsed beam centered at 800 nm. The output beam was split into pump and probe beams. The pump beam was sent to an optical parametric amplifier (OPerA Solo, Coherent Inc.) to obtain the desired wavelength of the pump beam. The probe beam was focused into a 4 mm CaF<sub>2</sub> crystal to generate a 350–750 nm white light continuum that was continuously translated with a linear stage (Newport MFACC) to avoid damage to the crystal. The probe beam was focused into the sample, while the pump was focused behind the sample, effectively resulting in a 2:3 beam size ratio that ensures

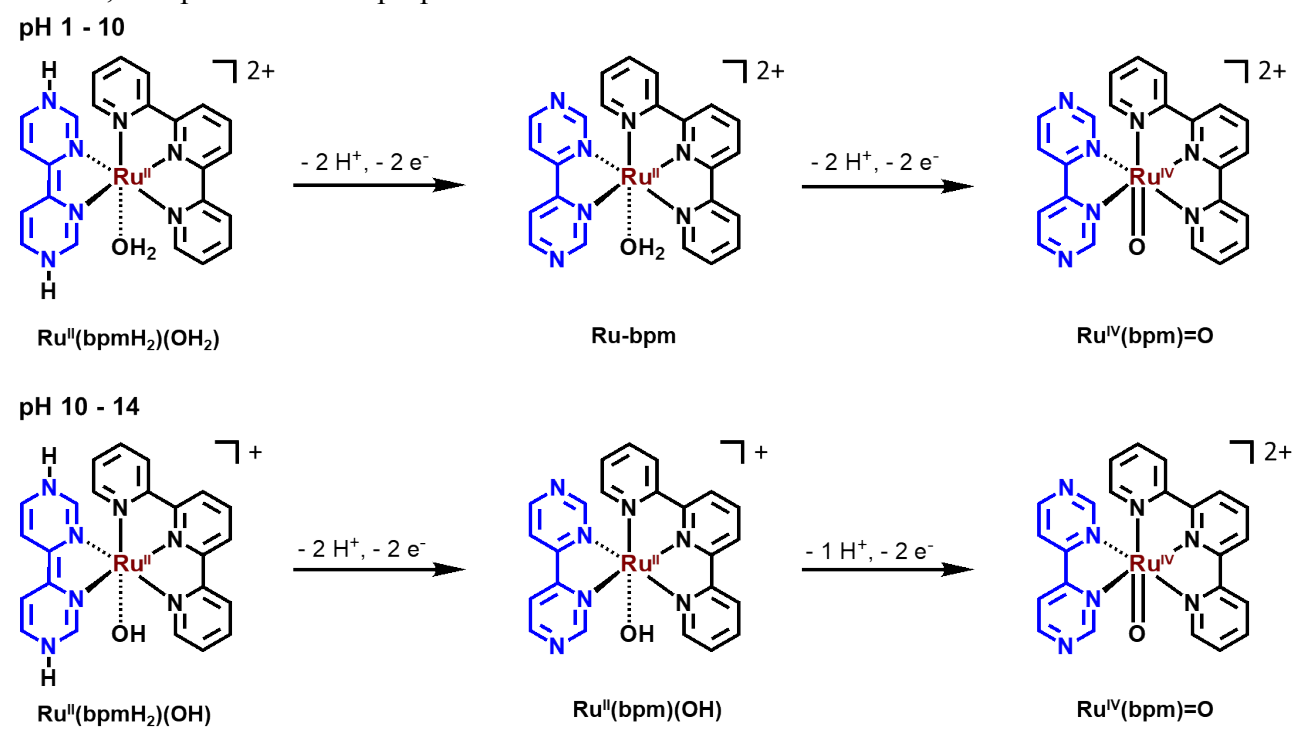
most efficient probing of the transient molecules. The angle between pump and probe polarizations was set to 54.7° to minimize the influence of molecular rotations on the ultrafast kinetics. After transmitting through the sample, the probe beam was directed into an optical fiber and input into a CCD spectrograph (Ocean Optics, Flame-S-UV-vis-ES). Data acquisition was performed using custom LabVIEW (National Instruments) software. Data processing (background subtraction, outlier removal, and averaging) was done in a custom LabView data processing program, while chirp correction was performed via CarpetView (Light Conversion). Global fitting analysis was performed using the global analysis function in CarpetView. Reported time constants with standard deviations were calculated as averages from three separate data sets. Numerous sequential models were tested, and their quality was evaluated based on the agreement between the calculated component spectra and the temporal evolution of the time-resolved spectra.

Computational methods. All calculations were performed using the Gaussian 16 software package<sup>26</sup> with resources of the Laboratory Computing Resource Center at Argonne National Laboratory. Geometry and frequency optimizations were performed at the B3LYP/6-31+g(d,p) level of theory<sup>27,28</sup> and LANL2DZ ECP basis set<sup>29</sup> for Ru center. with integral equation formalism variant of polarizable continuum model (iefpcm) for solvation effects.<sup>30</sup> Frequency calculations confirmed the structures obtained were at the local minima of their potential energy surfaces by resulting in the absence of imaginary frequencies. TD-DFT was performed to predict the spectra of Ru-bpm, Ru-bpmH<sup>+</sup>, and Ru-bpmH<sub>2</sub><sup>2+</sup>. DFT-based difference density calculations were performed to visualize the movement of charge on the molecule during the lowest energy, allowed transition. Natural transition orbitals<sup>31</sup> and charge transfer matrices<sup>32</sup> that were generated to better understand the nature of transitions in the UV-vis spectrum. To quantify charge transfer characters in a transition, we grouped the atoms in the molecule into four fragments: Ru, terpy, bpm and H<sub>2</sub>O. The charge transfer matrix elements are computed as a probability of each electronic state involved in the charge transfer event between fragments.

#### **Results and Discussion**

Electrochemistry of **Ru-bpm** reveals the proton-coupled redox activity of the Ru-center in the anodic region and of the bpm ligand in the cathodic region. This behavior is illustrated in cyclic voltammograms (CV) of **Ru-bpm** in aqueous medium, across a large pH region (Figures 1, S1, and S2). Representative CVs in acidic, neutral and basic solutions (Figure 1a) show the presence of a single reduction feature in the cathodic region (0 to -1 V vs. NHE, light blue traces) and a single oxidation feature in the anodic region (0 to +1.5 V vs NHE, dark blue traces). The cathodic feature is chemically reversible and exhibits pronounced pH-dependence. Similar behavior was observed previously for bipyrimidine-based nanographenes,<sup>33</sup> and is assigned to a two-electron, two-proton reduction of the bpm moiety to the corresponding dihydro-bipyrimidine (bpmH<sub>2</sub>) analog (Scheme 1). The bpm reduction feature exhibits a modest current enhancement in the cathodic scan for CVs collected at pH<2.0 (observable in the pH=2 CV, Figure 1a). This current increase indicates the presence of a catalytic process. The possibly of catalytic hydrogen-evolution was explored, but the headspace analysis of the electrolysis solution did not result in the detection of molecular hydrogen. The origin of this current enhancement is currently not understood. The

experimental CVs were used to construct the Pourbaix diagram for the bpm-based reduction feature (Figure 1b). Experimental data were fitted using a single Nernst equation for PCET<sup>34</sup> across the entire pH range, yielding a slope of -0.061 V/pH unit. This slope implies that the equal number of electrons and protons are transferred in the reduction process and is consistent with the two-electron, two-proton transfer proposed in Scheme 1.



**Scheme 1.** Scheme summarizing PCET processes in **Ru-bpm**. Ligand (bpm/bpmH<sub>2</sub>) reduction involves a two-electron, two-proton process in all pH regions. The proton stoichiometry associated with Ru-oxidation depends on the pH: a two-electron, two-proton (Ru=O/Ru(OH<sub>2</sub>)) oxidation occurs in the pH range 1-10, while a two-electron, one proton (Ru=O/Ru(OH)) oxidation occurs in the pH=10-14 range.

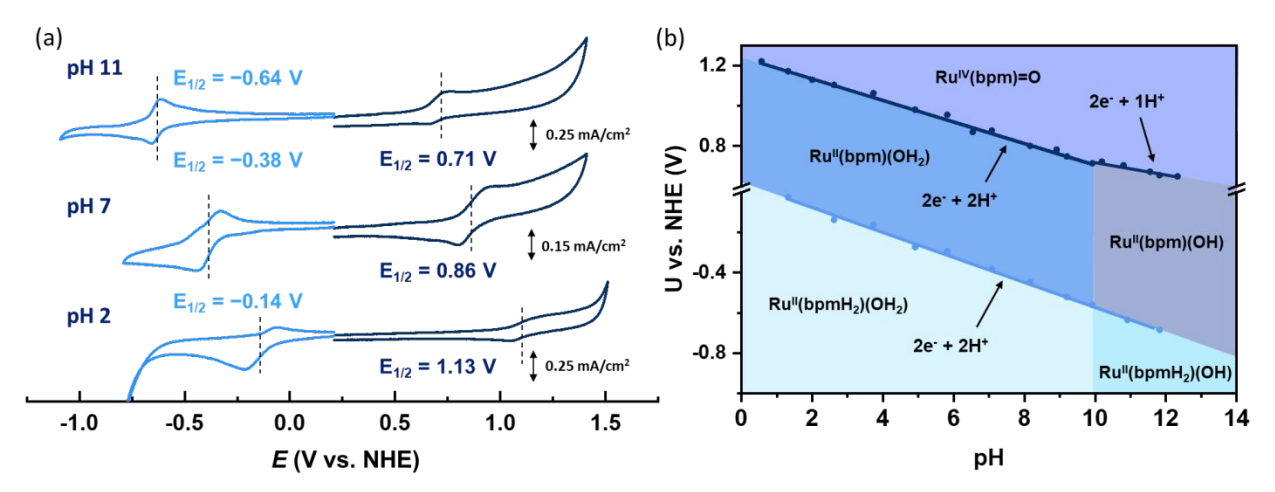


**Figure 1.** (a) Representative CVs of **Ru-bpm** taken at cathodic (light blue) and anodic (dark blue) potentials in the acidic (pH 2), neutral (pH 7) and basic (pH 11) pH regions and recorded at

a scan rate of 100 mV/s. (b) Pourbaix diagram of **Ru-bpm** showing the pH-dependence on bpm-centered reduction and Ru-centered oxidation features. The shaded areas and lines represent pH-potential regions where annotated species are stable and proton-coupled electron transfer occurs, respectively.

The peaks in the anodic region (0 to +1.5 V vs NHE) were assigned to Ru-based oxidations. Unlike many similar polypyridine-ligated Ru complexes, 35 where two separate Ru<sup>III</sup>/Ru<sup>II</sup> and Ru<sup>IV</sup>/Ru<sup>III</sup> features are observed, the **Ru-bpm** features only a single oxidation peak in the anodic region across all pH values (Figure 1a, dark blue traces). This oxidation feature is attributed to the two-electron Ru<sup>IV/II</sup> couple of **Ru-bpm**. The merge of two one-electron processes into one oxidation feature are the result of the bpm ligation. The increased  $\pi$ -backbonding and  $\sigma$ -donation of bpm ligand selectively stabilizes the Ru<sup>II</sup> and Ru<sup>IV</sup> states relative to Ru<sup>III</sup>. This consequence of this stabilization effect is the lower potential of the Ru<sup>IV/III</sup> couple relative to Ru<sup>III/II</sup>, leading to the presence of a single two-electron oxidation feature. Similar behavior was observed previously for other Rubased complexes with similar ligand structure.  $^{36-38}$  Plotting  $E_{1/2}$  for Ru<sup>IV/II</sup> against pH and fitting to the Nernst equation for PCET reveals two different regions (Figure 1b). The transition between two regions occurs at pH=9.9 where the deprotonation of the agua ligand is expected to occur. <sup>36,39</sup> At pH<10, the data were fit to a Nernst equation with the slope of -0.054 V/pH unit, which is consistent with the two-proton two-electron conversion from [Ru<sup>II</sup>-OH<sub>2</sub>]<sup>2+</sup> to [Ru<sup>IV</sup>=O]<sup>2+</sup> (Scheme 1). At pH>10, the slope is reduced to -0.026 V/pH unit, corresponding to the one-proton twoelectron conversion from [Ru<sup>II</sup>-OH]<sup>+</sup> to [Ru<sup>IV</sup>=O]<sup>2+</sup> (Scheme 1).

The electronic transitions in **Ru-bpm** were studied using pH-dependent steady-state UV/Vis absorption spectroscopy. The absorption spectra of **Ru-bpm** are pH-independent at pH>1 and consist of one absorption bands in the visible range, centered at  $\lambda$ =520 nm (Figure 2a). As the pH is lowered below pH=1, the absorption band shifts to the red. The new intermediate is detected at pH=-0.73, with absorption at centered at  $\lambda$  590 nm, while further acidification to pH=-0.88, leads to the formation of new product that absorbs at  $\lambda$ =680 nm. These spectral changes were assigned to the stepwise protonation of the uncoordinated N-centers on the bpm ligand to form **Ru-bpmH**<sup>+</sup> and Ru-bpmH<sub>2</sub><sup>2+</sup> species. The associated pKa values were determined to be pKa<sub>1</sub>=-0.7 and pKa<sub>2</sub>=-0.8 (Figure S3, Supp Info) and the value are in the agreement with the previously published pKa values of similar Ru-bipyrimidine complexes. <sup>21,40</sup> These experimental spectral changes are in excellent agreement with the calculated electronic transitions of Ru-bpm, Ru-bpmH<sup>+</sup> and Ru**bpmH**<sub>2</sub><sup>2+</sup> (Figure 2b, calculation details are shown in the Supplementary Material), which predict the visible absorption bands for Ru-bpm, Ru-bpmH<sup>+</sup> and Ru-bpmH<sub>2</sub><sup>2+</sup> to appear at 470, 615 and 730 nm, respectively. These absorption bands were evaluated using difference density plots (Figure 2c) and show that, in each case, the electronic density shifts from Ru and terpy units toward the bpm moiety.

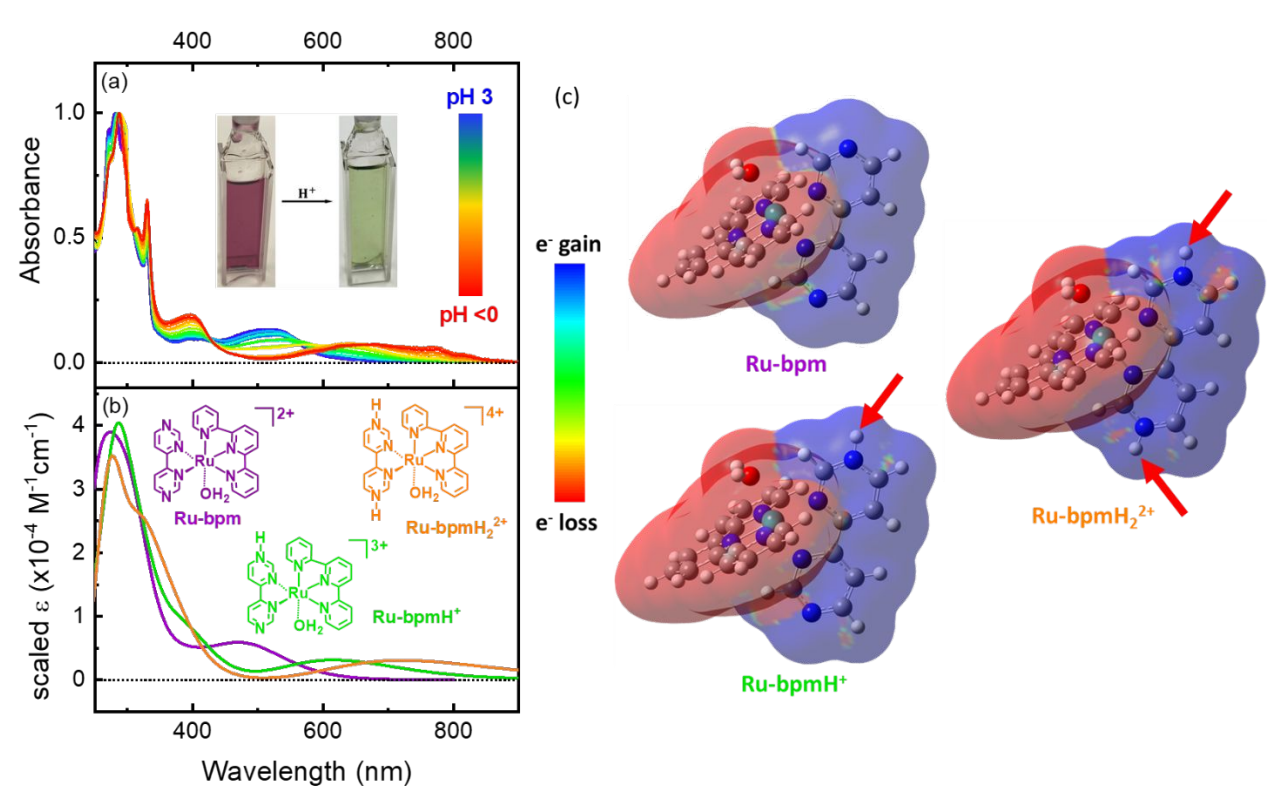


**Figure 2.** (a) Steady-state UV-vis absorption spectra of aqueous **Ru-bpm** solutions at various pH values. Inset shows the color change of **Ru-bpm** at pH=7 and when protonated at pH <0, indicating a substantial shift in the energy of the MLCT band. (b) TD-DFT calculated spectra of **Ru-bpm** in its unprotonated (violet), singly protonated (green), and doubly protonated (orange) forms. Calculations were performed at the B3LYP/6-31+G(d,p) level of theory with water solvation modeled by a polarizable continuum (iefpcm); c) Difference density (DD) plots of the model compounds showing the sites of charge accumulation (blue) and depletion (red) in the lowest energy bright excited states for **Ru-bpm, Ru-bpmH**<sup>+</sup> and **Ru-bpmH**<sub>2</sub><sup>2+</sup>. Protonated sites on **Ru-bpmH**<sup>+</sup> and **Ru-bpmH**<sub>2</sub><sup>2+</sup> are indicated with red arrows.

Detailed assignment of the three lowest-energy electronic transitions ( $S_1$ ,  $S_2$  and  $S_3$ ) of **Ru-bpm** was achieved using charge-transfer matrix calculations. Calculated transition wavelengths and the orbitals involved in each transition are shown in Figure 3. The highest contribution to each transition is attributed to metal-to-ligand charge transfer (MLCT) transitions:  $S_1$  and  $S_2$  states are associated with the charge accumulation at the bpm ligand ( $Ru \rightarrow bpm$  MLCT state), while the  $S_3$  state is associated with the charge accumulation at the terpy ligand ( $Ru \rightarrow terpy$  MLCT state). The lower energy of the  $Ru \rightarrow bpm$  MLCT states relative to  $Ru \rightarrow terpy$  states is consistent with better electron-accepting ability of the N-rich bpm ligand relative to terpy ligands. Each of the three transitions also involves a small contribution due to ligand-associated transitions, such as ligand-centered (LC) bpm  $\rightarrow$  bpm and terpy  $\rightarrow$  terpy transitions and intra-ligand charge transfer (ILCT) terpy  $\rightarrow$  bpm transitions. Finally, the  $S_3$  state also exhibits a small contribution from the  $Ru \rightarrow Ru$  metal-centered (MC) transitions. The presence of these low-energy MC states is likely associated with the terpy ligands, which are known to have a small bite angle, resulting in inefficient ligand field induced splitting of metal d-orbitals. The oscillator strengths of  $S_1$  (f=0.0013),  $S_2$  (f=0.1144)

and  $S_3$  (f=0.0097) transitions indicate that the excitation into the lowest-energy transition populated predominantly the  $S_3$  state.

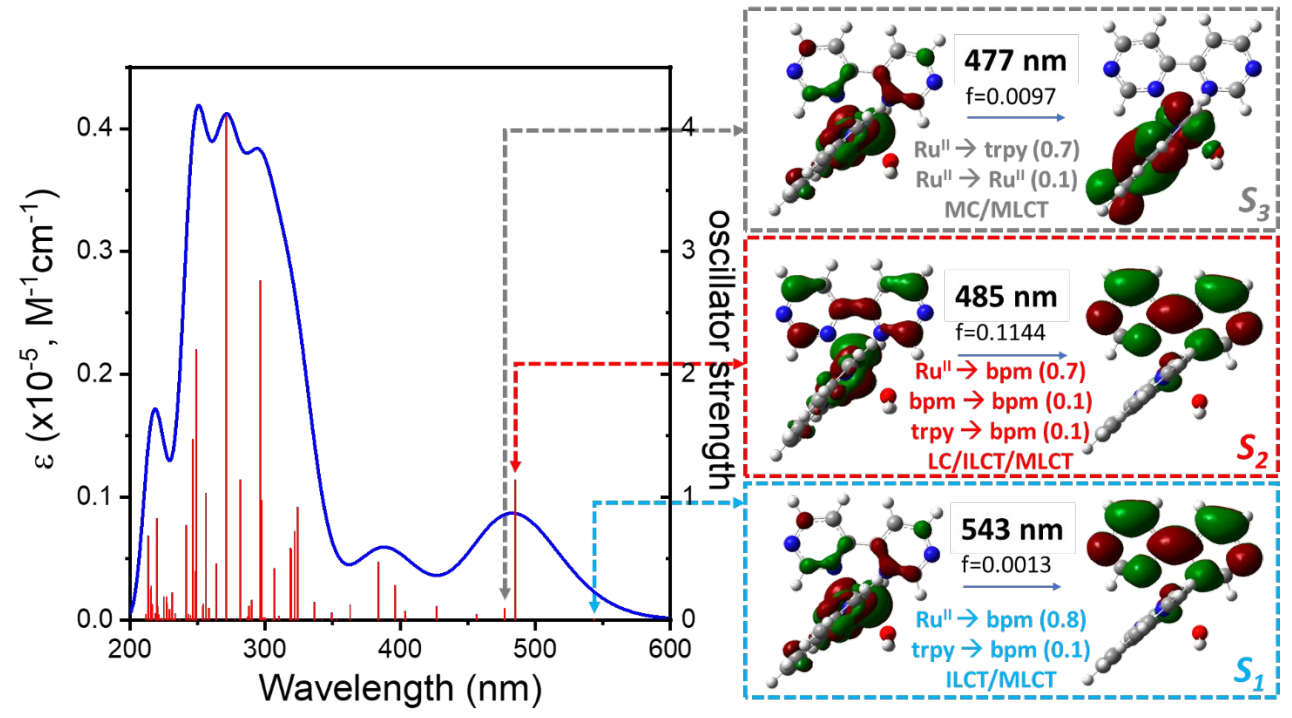


**Figure 3**. Electronic transition wavelengths calculated for **Ru-bpm** at the B3LYP/6-31+G(d,p) level of theory. Three lowest energy transitions (at 477, 485 and 543 nm) were characterized using charge-transfer matrix calculations and the orbitals involved in each transition are as follows:  $S_0$  transition is composed of Ru  $\rightarrow$  bpm MLCT (77%) and terpy  $\rightarrow$  bpy ILCT (12%) transitions;  $S_1$  transition is composed of Ru  $\rightarrow$  bpm MLCT (68%), bpm  $\rightarrow$  bpm LC (12%) and terpy  $\rightarrow$  bpy ILCT (12%) transitions;  $S_2$  transition is composed of Ru  $\rightarrow$  terpy MLCT (70%), terpy  $\rightarrow$  terpy LC (12%) and Ru  $\rightarrow$  Ru MC (12%) transitions

To better understand the pH-dependent photophysics of **Ru-bpm**, we employed femtosecond transient absorption (fsTA) spectroscopy (Figure 4). At pH=7 (Figure 4a), transient spectra consist of the ground state bleach in the 500-650 nm range and excited-state absorption with maximum at 350 nm. These spectral features are indicative of the Ru  $\rightarrow$  bpm  $^3$ MLCT state with the band at 350 nm assigned to the absorption by the reduced bpm moiety. This absorption band is red-shifted relative to the bpm-centered absorption of the molecule in the ground state (which appears at 350 nm, Figure 2a), as expected for the increased electronic density on bpm upon the formation of the  $^3$ MLCT states.  $^{42,43}$  Furthermore, the assignment of  $^3$ MLCT state is consistent with the DFT-predicted Ru  $\rightarrow$  bpm MLCT transition at 485 nm (Figure 3). The observed transients were found to decay biexponentially with lifetimes  $\tau_1$ =4 ps,  $\tau_2$ =65 ps. Such short excited-state decay in transition metal complexes is often associated with the involvement of MC transitions that are known to undergo fast excited state deactivation to the ground state or photochemical ligand loss.  $^{44-47}$  Since the low-lying metal-centered (MC) transition is predicted by DFT to appear at 477 nm (0.04 eV above the photogenerated  $^3$ MLCT state) it is quite possible that the observed fast kinetics are associated with the thermally activated MLCT  $\rightarrow$  MC state

transition. However, we rule out this scenario for several reasons. First, the observed lifetimes appear to be too short for MC state mediation. A very similar compound,  $[Ru(bpy)(terpy)(H_2O)]^{2+}$ , was found to exhibit an excited state lifetime of 270 ps, which was assigned to the mediation by MC states whose energy is lowered due to the small bite angle of the terpy ligand.<sup>41</sup> Thus, if the same mediation took place in **Ru-bpm**, the observed decay would be an order of magnitude slower than the observed. Second, the excited-state decay of **Ru-bpm** exhibits a large kinetic isotope effect (KIE) of 1.75 for the  $\tau_1$  component and 1.61 for  $\tau_2$  component (Figure 5). Such KIE is not expected for the MC-mediated deactivation. As a matter of fact, the inverse isotope effect was observed due to the stabilization effects caused by the aqua ligand.<sup>41</sup> Based on these arguments, we conclude that the fast excited-state decay in **Ru-bpm** is associated with another process, likely involving the contribution from the solvent.

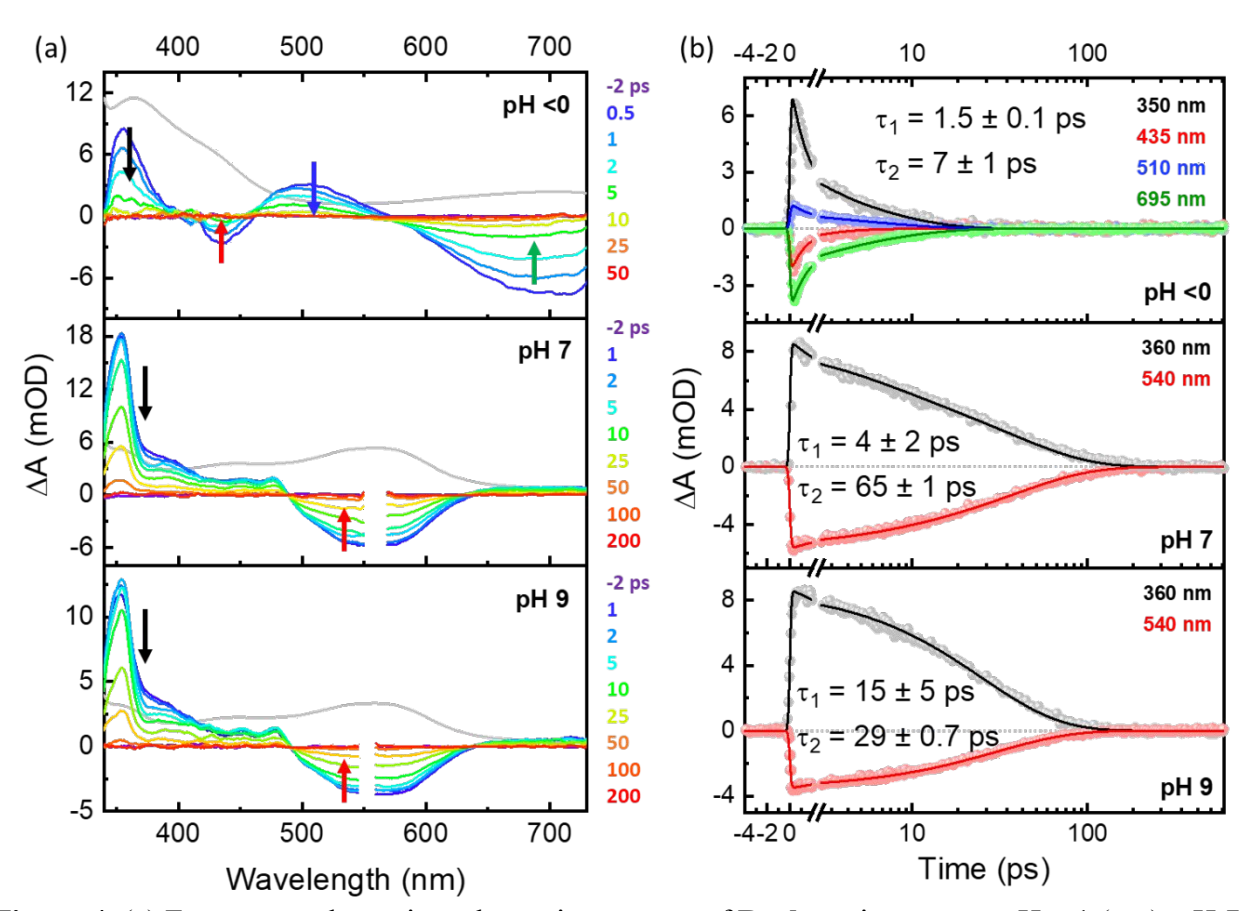


**Figure 4.** (a) Femtosecond transient absorption spectra of **Ru-bpm** in water at pH=-1 (top), pH 7 (middle), and pH 9 (bottom). Steady-state UV-vis spectra are overlaid in light grey. (b) Corresponding kinetic traces at selected wavelengths with data plotted as dots and fits, derived from target analysis using the A $\rightarrow$ B $\rightarrow$ GS (ground state) model, plotted as curves. Samples at pH =-1 were excited at 700 nm while samples at pH 7 and 9 were excited at 550 nm.

The presence of KIE hints at a possibility of excited-state proton transfer (ESPT) as the quenching mechanism for **Ru-bpm**. Similar ESPT processes were observed previously in Ru-bipyrazine complexes and have been assigned to the excited-state protonation of the bpm ligand.<sup>24</sup> This behavior is consistent with the increased basicity of non-coordinated N atoms in Ru  $\rightarrow$  bpm MLCT

excited states and similar effect is expected to occur in **Ru-bpm**. The excited-state protonation of the bpm ligand at pH=7 is thermodynamically favorable: our Förster cycle analysis predicts that the pKa value of protonated bpm shifts from p $K_a=-0.7$  in the ground state to p $K_a^*=6.15$  in the MLCT state (Eq. S1, Supp Info). If such protonation event occurred adiabatically, excited-state dynamics would be controlled by the excited-state lifetime of the protonated Ru(bpmH<sup>+</sup>), which we evaluated by measuring transient absorption spectra at pH=-1, where the ground-state protonation of bpm ligands is expected to occur (Figure 4). The transient absorption signal exhibits a bleach in the 550-800 nm range, consistent with the red shift of the MLCT absorption band upon protonation (Figure 2). Additional excited-state absorption bands appear at 350 and 500 nm and the overall signal decays biexponentially with lifetimes of  $\tau_1$ =1.5 and  $\tau_2$ =7 ps. Given that the excited state of **Ru-(bpmH**<sup>+</sup>) is indeed quite short-lived, the adiabatic excited-state protonation of **Ru-bpm** is expected to result in the observed short-lived excited states. To test the possibility that the ESPT mechanism is taking place, we collected transient absorption spectra of **Ru-bpm** at pH=9 (Figure 4). This pH value was selected because it is more basic than the pKa\*=6.15 value estimated for **Ru-bpm**. If ESPT were indeed taking place, the excited-state lifetime of **Ru-bpm** was expected to become significantly longer in the basic pH region, where the solvent is insufficiently acidic to protonate bpm ligands. Similar suppression of ESPT was observed in other Ru-bipyrimidine complexes in basic solutions, 48-50 resulting in detectable emission from 3MLCT state of the unprotonated complex. To our surprise, we found that the spectral features and kinetic traces obtained for **Ru-bpm** at pH=9 are quite similar to those obtained at pH=7, clearly eliminating the possibility that the ESPT is involved as the quenching mechanism for the **Ru-bpm** excited state.

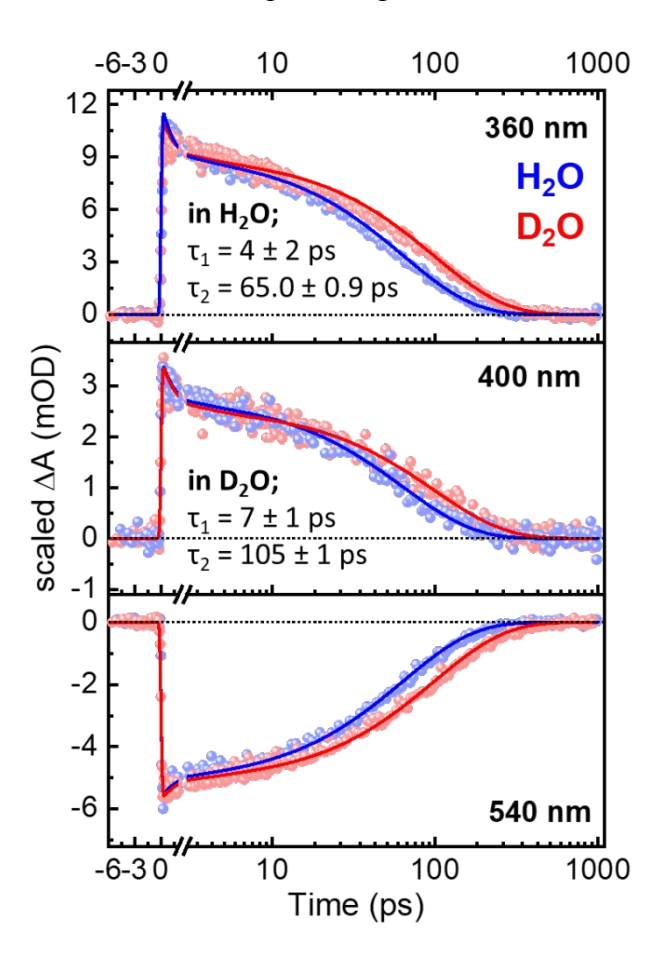


**Figure 5.** Kinetic traces of **Ru-bpm** at pH=7 in H<sub>2</sub>O (blue) and D<sub>2</sub>O (red) at 360 nm (top), 400 nm (middle), and 540 nm (bottom). Lifetimes calculated from target analysis are given in the inset.

The pH-dependent behavior of **Ru-bpm** is very similar to that observed previously for Ru and Os complexes with dipyridophenazine (dppz) ligands. 51-53 For example, Ru-dppz complexes were found to exhibit short excited-state lifetimes in water, while a significant increase in the lifetimes was observed in acetonitrile and other non-aqueous media.<sup>51</sup> This light switching behavior found application in biosensing of DNA and other biomolecules.<sup>52,53</sup> Mechanistically, the short excited state lifetimes observed in aqueous media were found to be insensitive to the pH changes, even though significant kinetic isotope effect was observed.<sup>51</sup> This behavior was hypothesized to occur due to the formation of MLCT states with strong hydrogen bonds between aza centers of the dppz radical anion and the water molecules. Optical transient absorption measurements showed that such hydrogen-bonded complex forms within several picoseconds, a timescale associated with water reorganization dynamics,<sup>52</sup> while the time-resolved infrared measurements provided direct evidence for the hydrogen-bonded complex through their vibrational signatures.<sup>54</sup> While strong experimental evidence exists that the hydrogen-bonded complex is involved in the fast excitedstate deactivation of Ru-complexes with dppz ligands, it is still not clear what is the mechanism of increased rates of nonradiative decay in these adducts. Based on the observed strong coupling of the vibrational modes of the dppz ligand and hydrogen-bonded water, it was hypothesized that fast vibrational energy transfer to the solvent causes the observed short excited-state lifetimes.<sup>54</sup>

It is highly likely that the hydrogen-bonded complex between **Ru-bpm** in its  ${}^3MLCT$  state and the solvent molecules causes the observed short excited-state decay in our system. To investigate this hypothesis further, we collected the transient absorption spectra of **Ru-bpm** in acetonitrile, where hydrogen-bonded complexation was not expected to occur. Results of this experiment are summarized in Figure 6 and show that both lifetime components increased from  $\tau_1$ =4 ps and  $\tau_2$ =65 ps in water to  $\tau_1$ =7 ps,  $\tau_2$ =76.5 ps in acetonitrile. These results show that the nature of the solvent plays an important role in the excited-state lifetimes. However, the observed lifetime increase is quite modest relative to that observed for dppz ligands, where a 2560-fold increase was reported. We assign this difference in behavior to the higher basicity of the aza moiety of bpm radical anion relative to that of the dppz analog. Due to smaller size of the bpm ligand relative to dppz, we expect that the aza moiety of the bpm radical anion formed in the  ${}^3MLCT$  state of **Ru-bpm** is a strong hydrogen-bond acceptor, capable of forming hydrogen bond adducts with acetonitrile. While acetonitrile is not as strong hydrogen bond donor as water, it has a reasonable hydrogen bond donating coefficients, hydrogen bond donor as water, it has a reasonable hydrogen bond donating coefficients, hydrogen bond donor as water, it has a reasonable hydrogen bond donating coefficients, hydrogen bond donor as water, it has a reasonable hydrogen bond donating coefficients, hydrogen bond donor as water, it has a reasonable hydrogen bond donating coefficients, hydrogen bond adduct.

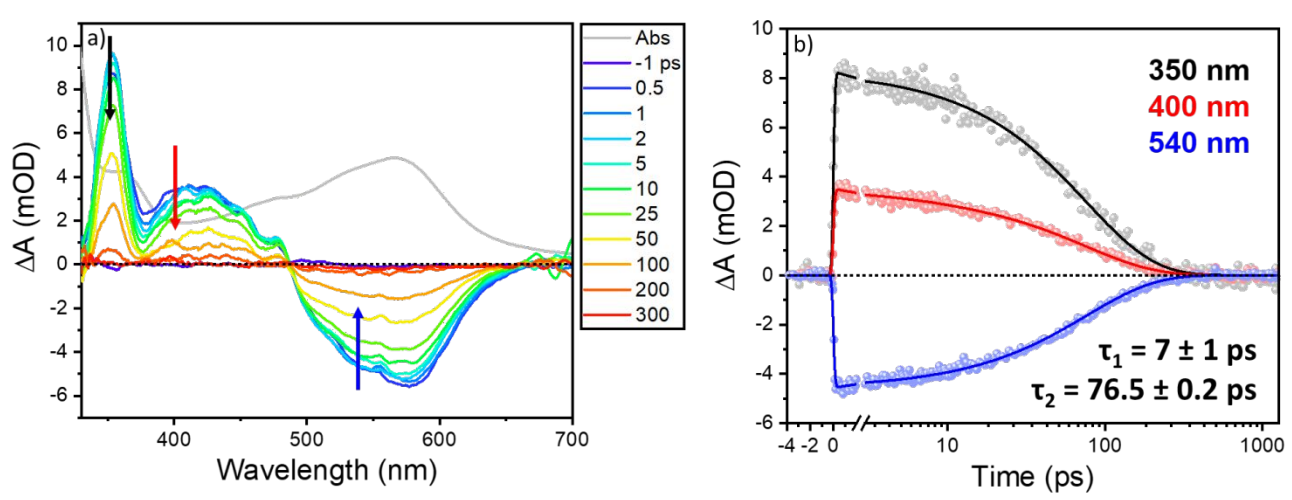
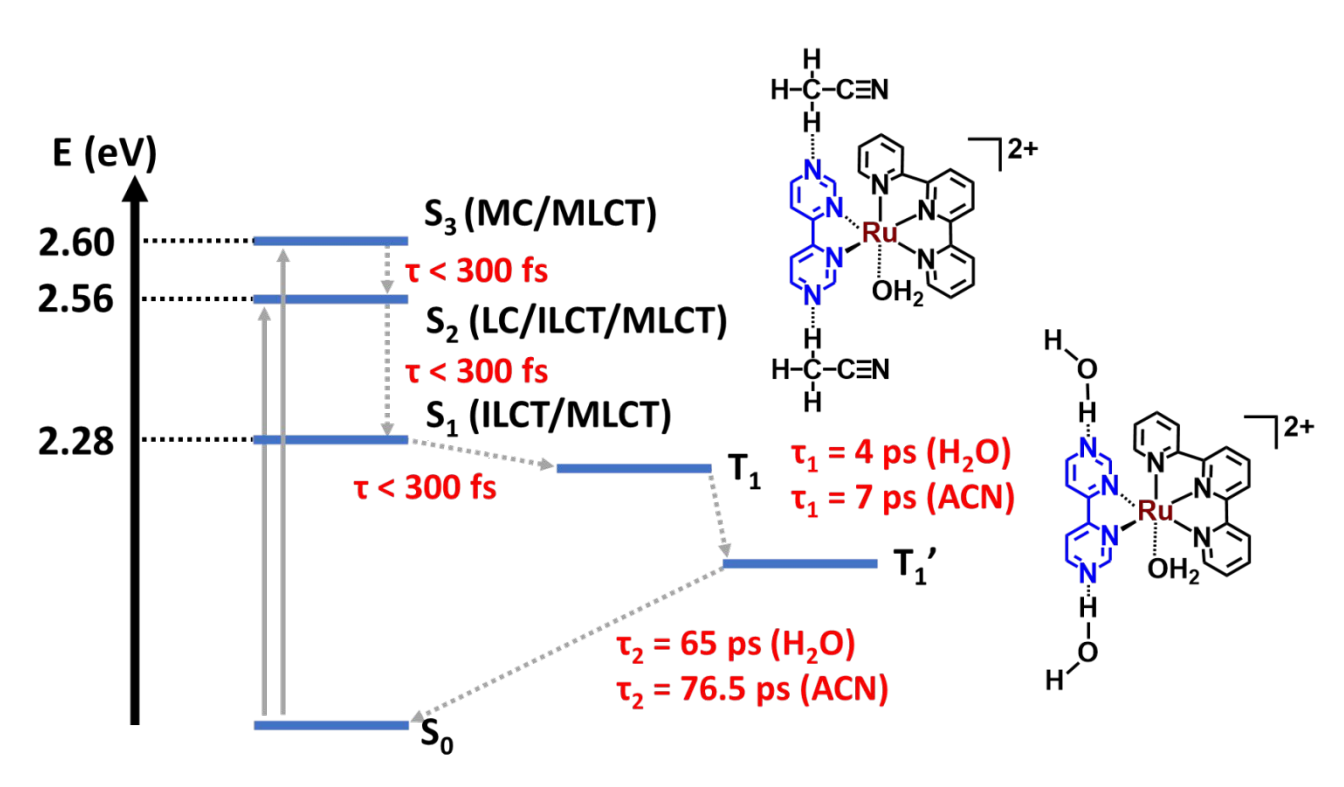


**Figure 6.** (a) Difference absorption spectra and (b) kinetic trace plots for the fsTA measurement of **Ru-bpm** in anhydrous acetonitrile excited at 550 nm.

Based on our experimental findings and the previous literature on similar complexes, we propose the Jablonski diagram shown in Scheme 2 to describe the excited state behavior of  $\mathbf{Ru\text{-}bpm}$ . The excitation into the lowest energy absorption band is expected to populate  $S_2$  and  $S_3$  states of  $\mathbf{Ru\text{-}bpm}$ . The  $S_1$  state is not populated directly due to the low oscillator strength calculated for this transition (Figure 3). The nonradiative internal conversion and intersystem crossing from these states to the  $T_1$  state are expected to occur at timescales shorter than the 300 fs instrument response function of our setup. The  $T_1$  state is predominantly characterized by the  $Ru \to bpm$  MLCT character, based on the transition orbitals calculated for the corresponding  $S_1$  state. The experimentally observed  $\tau_1$  lifetime is assigned to the solvent reorganization dynamics around the photogenerated molecular dipole, and this reorganization also includes the specific hydrogenbonding interactions between the solvent molecules and the aza-based hydrogen bond donors of the bpm radical anion moiety. The  $T_1$ ' state of the molecule/solvent adduct then decays back to the ground state with lifetime  $\tau_2$ , and this fast nonradiative decay is likely associated with efficient vibrational energy transfer to the solvent, facilitated by the strong coupling of the vibrational modes of bpm moiety with those of the hydrogen-bonded solvent.



**Scheme 2**: Jablonski diagram describing the excited state dynamics of **Ru-bpm** in different solvents. Proposed structures of hydrogen-bonded T<sub>1</sub>' states are shown for water and acetonitrile solvation.

#### Conclusion

In summary, we present a study of the electronic properties of **Ru-bpm**, a complex that contains redox-active Ru and bipyrimidine moieties. We find that the electrochemical behavior of **Ru-bpm** is dominated by the proton-coupled oxidation of Ru<sup>II</sup>-aqua to the corresponding Ru<sup>IV</sup>-oxo species and the proton-coupled reduction of bpm to bpmH<sub>2</sub>. The electronic transitions of **Ru-bpm** were found to be dominated by MLCT transitions with resonant frequencies in the visible region. We also find that **Ru-bpm** exhibits short excited-state lifetime and this behavior is attributed to the formation of a hydrogen-bonded adduct between the solvent and <sup>3</sup>MLCT state of **Ru-bpm**. Due to low solubility, the photophysical studies of **Ru-bpm** could not be performed in solvents with poor hydrogen-bond donating abilities (such as benzene). However, we postulate that the excited-state lifetime would exhibit an additional increase in such solvents, leading to interesting light switching behavior.

#### **Supporting Information**

Details on general methods, synthesis, characterization, steady-state spectroscopy, transient absorption spectroscopy, and computational methods. This material is available free of charge via the Internet at <a href="https://pubs.acs.org">https://pubs.acs.org</a>.

### Acknowledgments

This work is supported by the U.S. Department of Energy (DOE), Office of Science, Office of Basic Energy Science, Division of Chemical Sciences, Geosciences and Biosciences, through Argonne National Laboratory under Contract No. DE-AC02-06CH11357. K.D.G. also acknowledges the support provided by National Science Foundation (Grant Number 1954298). We also thank the Laboratory Computing Resource Center at Argonne National Laboratory for providing some of the computational resources used in this study.

#### References

- (1) *Photochemistry and Photophysics of Coordination Compounds I*; Balzani, V., Campagna, S., Eds.; Topics in Current Chemistry; Springer Berlin Heidelberg: Berlin, Heidelberg, 2007; Vol. 280. https://doi.org/10.1007/978-3-540-73347-8.
- (2) Knoll, J. D.; Albani, B. A.; Turro, C. New Ru(II) Complexes for Dual Photoreactivity: Ligand Exchange and <sup>1</sup> O <sub>2</sub> Generation. *Acc. Chem. Res.* **2015**, *48* (8), 2280–2287. https://doi.org/10.1021/acs.accounts.5b00227.
- (3) McCusker, J. K. Femtosecond Absorption Spectroscopy of Transition Metal Charge-Transfer Complexes. *Acc. Chem. Res.* **2003**, *36* (12), 876–887. https://doi.org/10.1021/ar030111d.
- (4) Gaynor, J. D.; Sandwisch, J.; Khalil, M. Vibronic Coherence Evolution in Multidimensional Ultrafast Photochemical Processes. *Nat. Commun.* **2019**, *10* (1), 5621. https://doi.org/10.1038/s41467-019-13503-9.
- (5) Yeh, A. T.; Shank, C. V.; McCusker, J. K. Ultrafast Electron Localization Dynamics Following Photo-Induced Charge Transfer. *Science* **2000**, *289* (5481), 935–938. https://doi.org/10.1126/science.289.5481.935.
- (6) Foxon, S. P.; Alamiry, M. A. H.; Walker, M. G.; Meijer, A. J. H. M.; Sazanovich, I. V.; Weinstein, J. A.; Thomas, J. A. Photophysical Properties and Singlet Oxygen Production by Ruthenium(II) Complexes of Benzo[ i ]Dipyrido[3,2- a:2',3'- c ]Phenazine: Spectroscopic and TD-DFT Study. *J. Phys. Chem. A* 2009, 113 (46), 12754–12762. https://doi.org/10.1021/jp906716g.
- (7) Kozlov, D. V.; Tyson, D. S.; Goze, C.; Ziessel, R.; Castellano, F. N. Room Temperature Phosphorescence from Ruthenium(II) Complexes Bearing Conjugated Pyrenylethynylene Subunits. *Inorg. Chem.* **2004**, *43* (19), 6083–6092. https://doi.org/10.1021/ic049288+.
- (8) Sauvage, J. P.; Collin, J. P.; Chambron, J. C.; Guillerez, S.; Coudret, C.; Balzani, V.; Barigelletti, F.; De Cola, L.; Flamigni, L. Ruthenium(II) and Osmium(II) Bis(Terpyridine) Complexes in Covalently-Linked Multicomponent Systems: Synthesis, Electrochemical Behavior, Absorption Spectra, and Photochemical and Photophysical Properties. *Chem. Rev.* **1994**, *94* (4), 993–1019. https://doi.org/10.1021/cr00028a006.
- (9) Winkler, J. R.; Netzel, T. L.; Creutz, C.; Sutin, N. Direct Observation of Metal-to-Ligand Charge-Transfer (MLCT) Excited States of Pentaammineruthenium(II) Complexes. *J. Am. Chem. Soc.* **1987**, *109* (8), 2381–2392. https://doi.org/10.1021/ja00242a023.
- (10) Hecker, C. R.; Gushurst, Ann. K. I.; McMillin, D. R. Phenyl Substituents and Excited-State Lifetimes in Ruthenium(II) Terpyridyls. *Inorg. Chem.* **1991**, *30* (3), 538–541. https://doi.org/10.1021/ic00003a037.

- Juris, A.; Balzani, V.; Barigelletti, F.; Campagna, S.; Belser, P.; von Zelewsky, A. Ru(II) Polypyridine Complexes: Photophysics, Photochemistry, Eletrochemistry, and Chemiluminescence. *Coord. Chem. Rev.* **1988**, *84*, 85–277. https://doi.org/10.1016/0010-8545(88)80032-8.
- (12) Jakubikova, E.; Chen, W.; Dattelbaum, D. M.; Rein, F. N.; Rocha, R. C.; Martin, R. L.; Batista, E. R. Electronic Structure and Spectroscopy of [Ru(Tpy) 2 ] <sup>2+</sup>, [Ru(Tpy)(Bpy)(H 2 O)] <sup>2+</sup>, and [Ru(Tpy)(Bpy)(Cl)] <sup>+</sup>. *Inorg. Chem.* **2009**, *48* (22), 10720–10725. https://doi.org/10.1021/ic901477m.
- (13) Abrahamsson, M.; Jäger, M.; Österman, T.; Eriksson, L.; Persson, P.; Becker, H.-C.; Johansson, O.; Hammarström, L. A 3.0 Ms Room Temperature Excited State Lifetime of a Bistridentate Ru <sup>II</sup> –Polypyridine Complex for Rod-like Molecular Arrays. *J. Am. Chem. Soc.* **2006**, *128* (39), 12616–12617. https://doi.org/10.1021/ja064262y.
- (14) Brown, D. G.; Sanguantrakun, N.; Schulze, B.; Schubert, U. S.; Berlinguette, C. P. Bis(Tridentate) Ruthenium—Terpyridine Complexes Featuring Microsecond Excited-State Lifetimes. *J. Am. Chem. Soc.* **2012**, *134* (30), 12354–12357. https://doi.org/10.1021/ja3039536.
- (15) Hicks, C.; Ye, G.; Levi, C.; Gonzales, M.; Rutenburg, I.; Fan, J.; Helmy, R.; Kassis, A.; Gafney, H. D. Excited-State Acid–Base Chemistry of Coordination Complexes. *Coord. Chem. Rev.* **2001**, *211* (1), 207–222. https://doi.org/10.1016/S0010-8545(00)00279-4.
- (16) Lennox, J. C.; Kurtz, D. A.; Huang, T.; Dempsey, J. L. Excited-State Proton-Coupled Electron Transfer: Different Avenues for Promoting Proton/Electron Movement with Solar Photons. *ACS Energy Lett.* **2017**, *2* (5), 1246–1256. https://doi.org/10.1021/acsenergylett.7b00063.
- (17) O'Donnell, R. M.; Sampaio, R. N.; Li, G.; Johansson, P. G.; Ward, C. L.; Meyer, G. J. Photoacidic and Photobasic Behavior of Transition Metal Compounds with Carboxylic Acid Group(s). *J. Am. Chem. Soc.* **2016**, *138* (11), 3891–3903. https://doi.org/10.1021/jacs.6b00454.
- (18) Das, S.; Saha, D.; Karmakar, S.; Baitalik, S. Effect of PH on the Photophysical and Redox Properties of a Ruthenium(II) Mixed Chelate Derived from Imidazole-4,5-Dicarboxylic Acid and 2,2'-Bipyridine: An Experimental and Theoretical Investigation. *J. Phys. Chem. A* **2012**, *116* (21), 5216–5226. https://doi.org/10.1021/jp300820p.
- (19) Peterson, S. H.; Demas, J. N. Excited State Acid-Base Reactions of Transition Metal Complexes: Dicyanobis(2,2'-Bipyridine) Ruthenium(III) in Aqueous Acid. *J. Am. Chem. Soc.* **1976**, *98* (24), 7880–7881. https://doi.org/10.1021/ja00440a100.
- (20) Giordano, P. J.; Bock, C. R.; Wrighton, M. S. Excited State Proton Transfer of Ruthenium(II) Complexes of 4,7-Dihydroxy-1,10-Phenanthroline. Increased Acidity in the Excited State. *J. Am. Chem. Soc.* **1978**, *100* (22), 6960–6965. https://doi.org/10.1021/ja00490a032.
- (21) Nazeeruddin, M. K.; Kalyanasundaram, K. Acid-Base Behavior in the Ground and Excited States of Ruthenium(II) Complexes Containing Tetraimines or Dicarboxybipyridines as Protonatable Ligands. *Inorg. Chem.* **1989**, *28* (23), 4251–4259. https://doi.org/10.1021/ic00322a015.
- (22) Shimidzu, T.; Iyoda, T.; Izaki, K. Photoelectrochemical Properties of Bis(2,2'-Bipyridine)(4,4'-Dicarboxy-2,2'-Bipyridine)Ruthenium(II) Chloride. *J. Phys. Chem.* **1985**, *89* (4), 642–645. https://doi.org/10.1021/j100250a018.

- (23) Giordano, P. J.; Bock, C. R.; Wrighton, M. S.; Interrante, L. V.; Williams, R. F. X. Excited State Proton Transfer of a Metal Complex: Determination of the Acid Dissociation Constant for a Metal-to-Ligand Charge Transfer State of a Ruthenium(II) Complex. *J. Am. Chem. Soc.* **1977**, *99* (9), 3187–3189. https://doi.org/10.1021/ja00451a066.
- (24) Crutchley, R. J.; Kress, N.; Lever, A. B. P. Protonation Equilibria in Excited-State Tris(Bipyrazine)Ruthenium(II). *J. Am. Chem. Soc.* **1983**, *105* (5), 1170–1178. https://doi.org/10.1021/ja00343a016.
- (25) Fujihara, T.; Wada, T.; Tanaka, K. Syntheses and Electrochemical Properties of Ruthenium(II) Complexes with 4,4'-Bipyrimidine and 4,4'-Bipyrimidinium Ligands. *Inorganica Chim. Acta* **2004**, *357* (4), 1205–1212. https://doi.org/10.1016/j.ica.2003.10.015.
- (26) Frisch, M. J.; Trucks, G. W.; Schlegel, H. B.; Scuseria, G. E.; Robb, M. A.; Cheeseman, J. R.; Scalmani, G.; Barone, V.; Mennucci, B.; Petersson, G. A.; Nakatsuji, H.; Caricato, M.; Li, X.; Hratchian, H. P.; Izmaylov, A. F.; Bloino, J.; Zheng, G.; Sonnenberg, J. L.; Liang, W.; Hada, M.; Ehara, M.; Toyota, K.; Fukuda, R.; Hasegawa, J.; Ishida, M.; Nakajima, T.; Honda, Y.; Kitao, O.; Nakai, H.; Vreven, T.; Montgomery, Jr. J. A.; Peralta, J. E.; Ogliaro, F.; Bearpark, M.; Heyd, J. J.; Brothers, E.; Kudin, K. N.; Staroverov, V. N.; Keith, T.; Kobayashi, R.; Normand, J.; Raghavachari, K.; Rendell, A.; Burant, J. C.; Iyengar, S. S.; Tomasi, J.; Cossi, M.; Rega, N.; Millam, J. M.; Klene, M.; Knox, J. E.; Cross, J. B.; Bakken, V.; Adamo, C.; Jaramillo, J.; Gomperts, R.; Stratmann, R. E.; Yazyev, O.; Austin, A. J.; Cammi, R.; Pomelli, C.; Ochterski, J. W.; Martin, R. L.; Morokuma, K.; Zakrzewski, V. G.; Voth, G. A.; Salvador, P.; Dannenberg, J. J.; Dapprich, S.; Parandekar, P. V.; Mayhall, N. J.; Daniels, A. D.; Farkas, Ö.; Foresman, J. B.; Ortiz, J. V.; Cioslowski, J.; Fox, D. J. Gaussian Development Version Revision 1.02.
- (27) Becke, A. D. Density-Functional Exchange-Energy Approximation with Correct Asymptotic Behavior. *Phys. Rev. A* **1988**, *38* (6), 3098–3100. https://doi.org/10.1103/PhysRevA.38.3098.
- (28) Lee, C.; Yang, W.; Parr, R. G. Development of the Colle-Salvetti Correlation-Energy Formula into a Functional of the Electron Density. *Phys. Rev. B* **1988**, *37* (2), 785–789. https://doi.org/10.1103/PhysRevB.37.785.
- (29) Hay, P. J.; Wadt, W. R. *Ab Initio* Effective Core Potentials for Molecular Calculations. Potentials for the Transition Metal Atoms Sc to Hg. *J. Chem. Phys.* **1985**, *82* (1), 270–283. https://doi.org/10.1063/1.448799.
- (30) Tomasi, J.; Persico, M. Molecular Interactions in Solution: An Overview of Methods Based on Continuous Distributions of the Solvent. *Chem. Rev.* **1994**, *94* (7), 2027–2094. https://doi.org/10.1021/cr00031a013.
- (31) Martin, R. L. Natural Transition Orbitals. *J. Chem. Phys.* **2003**, *118* (11), 4775–4777. https://doi.org/10.1063/1.1558471.
- (32) Mewes, S. A.; Dreuw, A. Density-Based Descriptors and Exciton Analyses for Visualizing and Understanding the Electronic Structure of Excited States. *Phys. Chem. Chem. Phys.* **2019**, *21* (6), 2843–2856. https://doi.org/10.1039/C8CP07191H.
- (33) Zoric, M. R.; Askins, E. J.; Qiao, X.; Glusac, K. D. Strong Electronic Coupling of Graphene Nanoribbons onto Basal Plane of a Glassy Carbon Electrode. *ACS Appl. Electron. Mater.* **2021**, *3* (2), 854–860. https://doi.org/10.1021/acsaelm.0c00978.

- (34) Warren, J. J.; Tronic, T. A.; Mayer, J. M. Thermochemistry of Proton-Coupled Electron Transfer Reagents and Its Implications. *Chem. Rev.* **2010**, *110* (12), 6961–7001. https://doi.org/10.1021/cr100085k.
- (35) Takeuchi, K. J.; Thompson, M. S.; Pipes, D. W.; Meyer, T. J. Redox and Spectral Properties of Monooxo Polypyridyl Complexes of Ruthenium and Osmium in Aqueous Media. *Inorg. Chem.* **1984**, *23* (13), 1845–1851. https://doi.org/10.1021/ic00181a014.
- (36) Concepcion, J. J.; Jurss, J. W.; Templeton, J. L.; Meyer, T. J. One Site Is Enough. Catalytic Water Oxidation by [Ru(Tpy)(Bpm)(OH 2)] <sup>2+</sup> and [Ru(Tpy)(Bpz)(OH 2)] <sup>2+</sup>. *J. Am. Chem. Soc.* **2008**, *130* (49), 16462–16463. https://doi.org/10.1021/ja8059649.
- (37) Masllorens, E.; Rodríguez, M.; Romero, I.; Roglans, A.; Parella, T.; Benet-Buchholz, J.; Poyatos, M.; Llobet, A. Can the Disproportion of Oxidation State III Be Favored in Ru <sup>II</sup> –OH <sub>2</sub> /Ru <sup>IV</sup> O Systems? *J. Am. Chem. Soc.* **2006**, *128* (16), 5306–5307. https://doi.org/10.1021/ja057733+.
- (38) Dovletoglou, A.; Adeyemi, S. A.; Meyer, T. J. Coordination and Redox Chemistry of Substituted-Polypyridyl Complexes of Ruthenium. *Inorg. Chem.* **1996**, *35* (14), 4120–4127. https://doi.org/10.1021/ic9512587.
- (39) Huynh, M. H. V.; Meyer, T. J. Proton-Coupled Electron Transfer. *Chem. Rev.* **2007**, *107* (11), 5004–5064. https://doi.org/10.1021/cr0500030.
- (40) Kirsch-De Mesmaeker, A.; Jacquet, L.; Nasielski, J. Ruthenium(II) Complexes of 1,4,5,8-Tetraazaphenanthrene (TAP) and 2,2'-Bipyridine (Bpy). Ground- and Excited-State Basicities of Ru2+(Bpy)n(TAP)3-n (n = 0,1,2): Their Luminescence Quenching by Organic Buffers. *Inorg. Chem.* **1988**, *27* (24), 4451–4458. https://doi.org/10.1021/ic00297a023.
- (41) Hewitt, J. T.; Concepcion, J. J.; Damrauer, N. H. Inverse Kinetic Isotope Effect in the Excited-State Relaxation of a Ru(II)—Aquo Complex: Revealing the Impact of Hydrogen-Bond Dynamics on Nonradiative Decay. *J. Am. Chem. Soc.* **2013**, *135* (34), 12500–12503. https://doi.org/10.1021/ja4037498.
- (42) Barqawi, K.; Akasheh, T. S.; Parsons, B. J.; Beaumont, P. C. One-Electron Reduction of 2,2'-Bipyrimidine in Aqueous Solution. *J. Chem. Soc. Faraday Trans. 1 Phys. Chem. Condens. Phases* **1987**, *83* (11), 3415. https://doi.org/10.1039/f19878303415.
- (43) Wallin, S.; Davidsson, J.; Modin, J.; Hammarström, L. Femtosecond Transient Absorption Anisotropy Study on [Ru(Bpy) 3 ] <sup>2+</sup> and [Ru(Bpy)(Py) 4 ] <sup>2+</sup>. Ultrafast Interligand Randomization of the MLCT State. *J. Phys. Chem. A* **2005**, *109* (21), 4697–4704. https://doi.org/10.1021/jp0509212.
- (44) Wagenknecht, P. S.; Ford, P. C. Metal Centered Ligand Field Excited States: Their Roles in the Design and Performance of Transition Metal Based Photochemical Molecular Devices. *Coord. Chem. Rev.* 2011, 255 (5–6), 591–616. https://doi.org/10.1016/j.ccr.2010.11.016.
- (45) Wacholtz, W. M.; Auerbach, R. A.; Schmehl, R. H.; Ollino, M.; Cherry, W. R. Correlation of Ligand Field Excited-State Energies with Ligand Field Strength in (Polypyridine)Ruthenium(II) Complexes. *Inorg. Chem.* **1985**, *24* (12), 1758–1760. https://doi.org/10.1021/ic00206a009.
- (46) Strekas, T. C.; Gafney, H. D.; Tysoe, S. A.; Thummel, R. P.; Lefoulon, F. Resonance Raman Spectra and Excited-State Lifetimes for a Series of 3,3'-Polymethylene-2,2'-Bipyridine Complexes of Ruthenium(II). *Inorg. Chem.* **1989**, *28* (15), 2964–2967. https://doi.org/10.1021/ic00314a018.

- (47) Juban, E. A.; Smeigh, A. L.; Monat, J. E.; McCusker, J. K. Ultrafast Dynamics of Ligand-Field Excited States. *Coord. Chem. Rev.* 2006, 250 (13–14), 1783–1791. https://doi.org/10.1016/j.ccr.2006.02.010.
- (48) Rillema, D. P.; Allen, G.; Meyer, T. J.; Conrad, D. Redox Properties of Ruthenium(II) Tris Chelate Complexes Containing the Ligands 2,2'-Bipyrazine, 2,2'-Bipyridine, and 2,2'-Bipyrimidine. *Inorg. Chem.* **1983**, *22* (11), 1617–1622. https://doi.org/10.1021/ic00153a012.
- (49) Turro, C.; Bossmann, S. H.; Jenkins, Y.; Barton, J. K.; Turro, N. J. Proton Transfer Quenching of the MLCT Excited State of Ru(Phen)2dppz2+ in Homogeneous Solution and Bound to DNA. *J. Am. Chem. Soc.* **1995**, *117* (35), 9026–9032. https://doi.org/10.1021/ja00140a020.
- (50) Concepcion, J. J.; Brennaman, M. K.; Deyton, J. R.; Lebedeva, N. V.; Forbes, M. D. E.; Papanikolas, J. M.; Meyer, T. J. Excited-State Quenching by Proton-Coupled Electron Transfer. *J. Am. Chem. Soc.* **2007**, *129* (22), 6968–6969. https://doi.org/10.1021/ja069049g.
- (51) Olson, E. J. C.; Hu, D.; Hörmann, A.; Jonkman, A. M.; Arkin, M. R.; Stemp, E. D. A.; Barton, J. K.; Barbara, P. F. First Observation of the Key Intermediate in the "Light-Switch" Mechanism of [Ru(Phen) <sub>2</sub> Dppz] <sup>2+</sup>. *J. Am. Chem. Soc.* **1997**, *119* (47), 11458–11467. https://doi.org/10.1021/ja971151d.
- (52) Onfelt, B.; Lincoln, P.; Norden, B.; Baskin, J. S.; Zewail, A. H. Femtosecond Linear Dichroism of DNA-Intercalating Chromophores: Solvation and Charge Separation Dynamics of [Ru(Phen)2dppz]2+ Systems. *Proc. Natl. Acad. Sci.* **2000**, *97* (11), 5708–5713. https://doi.org/10.1073/pnas.100127397.
- (53) Holmlin, R. E.; Yao, J. A.; Barton, J. K. Dipyridophenazine Complexes of Os(II) as Red-Emitting DNA Probes: Synthesis, Characterization, and Photophysical Properties. *Inorg. Chem.* **1999**, *38* (1), 174–189. https://doi.org/10.1021/ic9808955.
- (54) Poynton, F. E.; Hall, J. P.; Keane, P. M.; Schwarz, C.; Sazanovich, I. V.; Towrie, M.; Gunnlaugsson, T.; Cardin, C. J.; Cardin, D. J.; Quinn, S. J.; Long, C.; Kelly, J. M. Direct Observation by Time-Resolved Infrared Spectroscopy of the Bright and the Dark Excited States of the [Ru(Phen) 2 (Dppz)] <sup>2+</sup> Light-Switch Compound in Solution and When Bound to DNA. *Chem. Sci.* **2016**, *7* (5), 3075–3084. https://doi.org/10.1039/C5SC04514B.
- (55) Hunter, C. A. Quantifying Intermolecular Interactions: Guidelines for the Molecular Recognition Toolbox. *Angew. Chem. Int. Ed.* **2004**, *43* (40), 5310–5324. https://doi.org/10.1002/anie.200301739.

# **TOC Graphic**

